

Transfinite mean value interpolation over polygons

Michael S. Floater*

Francesco Patrizi†

June 21, 2019

Abstract

Mean value interpolation is a method for fitting a smooth function to piecewise-linear data prescribed on the boundary of a polygon of arbitrary shape, and has applications in computer graphics and curve and surface modelling. The method generalizes to transfinite interpolation, i.e., to any continuous data on the boundary but a mathematical proof that interpolation always holds has so far been missing. The purpose of this note is to complete this gap in the theory.

Keywords: Mean value coordinates, mean value interpolation, transfinite interpolation.

1 Introduction

One of the main uses of generalized barycentric coordinates (GBCs) is to interpolate piecewise-linear data prescribed on the boundary of a polygon with a smooth function. This kind of barycentric interpolation has been used, for example, in computer graphics, as the basis for image warping, and in higher dimension, for mesh deformation.

One type of GBC that is frequently used for this is mean value (MV) coordinates due to a simple closed formula. MV coordinates have been studied extensively in various papers [3] but while they are simple to implement, a mathematical proof of interpolation seems surprisingly difficult. A proof for convex polygons is relatively simple and follows from the fact that MV coordinates are positive in this case. Interpolation for a convex polygon holds in fact for any positive barycentric coordinates; see [4]. For arbitrary polygons, a specific proof of interpolation for MV coordinates was derived in [6].

*Department of Mathematics, University of Oslo, Moltke Moes vei 35, 0851 Oslo, Norway, *email:* michael.f@math.uio.no

†SINTEF, PO Box 124 Blindern, 0314 Oslo, Norway, *email:* francesco.patrizi@sintef.no

The MV interpolant to piecewise-linear boundary data is based on integration with respect to angles around each chosen point inside the polygon. This construction extends in a natural way to any continuous boundary data thus providing a transfinite interpolant [7, 1]. Such interpolation could have various applications, one of which is its use as a building block for interpolants of higher order that also match derivative data on the boundary. However, there is currently no mathematical proof of interpolation in the transfinite setting in all cases, only numerical evidence. Like in the piecewise-linear case, when the polygon is convex, interpolation is easier to establish. In fact it was shown in [1] for more general domains, convex or otherwise, under the condition that the distance between the external medial axis of the domain and the domain boundary is strictly positive. This latter condition trivially holds for convex domains since there is no external medial axis in this case.

This still leaves open the question of whether MV interpolation really interpolates any continuous data on the boundary of an arbitrary polygon, and this is what we establish in this paper. The proof parallels that of [6] in that we treat interpolation at edge points and vertices separately: in Theorems 1 and 2 respectively. At the end of the paper we give two examples that numerically confirm the interpolation property.

In the future we would like to extend the proof of interpolation to 3D geometry such as volumes enclosed by triangular meshes [5, 7] but there does not seem to be any straightforward generalization of the proof in the 2D case, not even for piecewise-linear boundary data. It would also be interesting to establish transfinite interpolation over more general domains with weaker conditions on the shape of the boundary than those used in [1].

2 Definitions

Let $\Omega \subset \mathbb{R}^2$ be a polygon with vertices V and edges E . Suppose that $f : \partial\Omega \rightarrow \mathbb{R}$ is a continuous function on the boundary $\partial\Omega$. We define a function $g : \Omega \rightarrow \mathbb{R}$ as follows. For each edge $e \in E$, let \mathbf{n}_e denote the outward unit normal to e with respect to Ω , and for each point $\mathbf{x} \in \Omega$, let $h_e(\mathbf{x})$ be its signed distance to e ,

$$h_e(\mathbf{x}) = (\mathbf{y} - \mathbf{x}) \cdot \mathbf{n}_e,$$

for any $\mathbf{y} \in e$. We let $\tau_e(\mathbf{x}) \in \{-1, 0, 1\}$ be the sign of the distance,

$$\tau_e(\mathbf{x}) = \text{sgn}(h_e(\mathbf{x})).$$

Let SS_1 denote the unit circle in \mathbb{R}^2 . For $\mathbf{x} \in \Omega$, let $\widehat{e}(\mathbf{x}) \subset SS_1$ denote the circular arc on SS_1 formed by projecting e onto the unit circle centred at \mathbf{x} ,

$$\widehat{e}(\mathbf{x}) = \left\{ \frac{\mathbf{y} - \mathbf{x}}{\|\mathbf{y} - \mathbf{x}\|} : \mathbf{y} \in e \right\},$$

with $\|\cdot\|$ the Euclidean norm. This arc is just a point in the case that $\tau_e(\mathbf{x}) = 0$. Suppose $\tau_e(\mathbf{x}) \neq 0$. Then for each unit vector $\boldsymbol{\mu} \in \widehat{e}(\mathbf{x})$, let $\mathbf{y}_e(\mathbf{x}, \boldsymbol{\mu})$ be the unique

point of e such that

$$\frac{\mathbf{y}_e(\mathbf{x}, \boldsymbol{\mu}) - \mathbf{x}}{\|\mathbf{y}_e(\mathbf{x}, \boldsymbol{\mu}) - \mathbf{x}\|} = \boldsymbol{\mu},$$

and let

$$I_e(\mathbf{x}) = \int_{\hat{e}(\mathbf{x})} \frac{1}{\|\mathbf{y}_e(\mathbf{x}, \boldsymbol{\mu}) - \mathbf{x}\|} d\boldsymbol{\mu} > 0, \quad I_e(\mathbf{x}; f) = \int_{\hat{e}(\mathbf{x})} \frac{f(\mathbf{y}_e(\mathbf{x}, \boldsymbol{\mu}))}{\|\mathbf{y}_e(\mathbf{x}, \boldsymbol{\mu}) - \mathbf{x}\|} d\boldsymbol{\mu}.$$

In the case that $\tau_e(\mathbf{x}) = 0$, we define $I_e(\mathbf{x}) = I_e(\mathbf{x}; f) = 0$.

We now define

$$g(\mathbf{x}) = \mathcal{I}f(\mathbf{x}) = \sum_{e \in E} \tau_e(\mathbf{x}) I_e(\mathbf{x}; f) / \phi(\mathbf{x}), \quad (1)$$

where

$$\phi(\mathbf{x}) = \sum_{e \in E} \tau_e(\mathbf{x}) I_e(\mathbf{x}). \quad (2)$$

As shown in [2], if $e = [\mathbf{v}_1, \mathbf{v}_2]$ then

$$I_e(\mathbf{x}) = \tan(\alpha_e(\mathbf{x})/2) \left(\frac{1}{\|\mathbf{v}_1 - \mathbf{x}\|} + \frac{1}{\|\mathbf{v}_2 - \mathbf{x}\|} \right), \quad (3)$$

where $\alpha_e(\mathbf{x}) \in [0, \pi)$ is the angle at \mathbf{x} of the triangle $[\mathbf{x}, \mathbf{v}_1, \mathbf{v}_2]$. It was shown in [6] that $\phi(\mathbf{x}) > 0$ for all $\mathbf{x} \in \Omega$, and in the case that f is linear, g interpolates f .

3 Interpolation on an edge

Theorem 1 *Let \mathbf{y}_* be an interior point of some edge of $\partial\Omega$. Then $g(\mathbf{x}) \rightarrow f(\mathbf{y}_*)$ as $\mathbf{x} \rightarrow \mathbf{y}_*$ for $\mathbf{x} \in \Omega$.*

Proof. From the form of (1),

$$g(\mathbf{x}) - f(\mathbf{y}_*) = \sum_{e \in E} \tau_e(\mathbf{x}) I_e(\mathbf{x}; \tilde{f}) / \phi(\mathbf{x}),$$

where $\tilde{f}(\mathbf{y}) := f(\mathbf{y}) - f(\mathbf{y}_*)$ and therefore

$$|g(\mathbf{x}) - f(\mathbf{y}_*)| \leq \sum_{e \in E} I_e(\mathbf{x}; |\tilde{f}|) / \phi(\mathbf{x}). \quad (4)$$

Let $[\mathbf{v}_1, \mathbf{v}_2] \in E$ be the edge containing \mathbf{y}_* , as in Figure 1. Let $\epsilon > 0$. By the continuity of f , there is some δ , where

$$0 < \delta < \min\{\|\mathbf{v}_1 - \mathbf{y}_*\|, \|\mathbf{v}_2 - \mathbf{y}_*\|\},$$

such that if $\mathbf{y} \in [\mathbf{v}_1, \mathbf{v}_2]$ and $\|\mathbf{y} - \mathbf{y}_*\| \leq \delta$ then $|f(\mathbf{y}) - f(\mathbf{y}_*)| < \epsilon$. Let $\mathbf{y}_j \in [\mathbf{y}_*, \mathbf{v}_j]$, $j = 1, 2$, be the point such that $\|\mathbf{y}_j - \mathbf{y}_*\| = \delta$, and let $e_0 = [\mathbf{y}_1, \mathbf{y}_2]$. Then,

$$\sum_{e \in E} I_e(\mathbf{x}; |\tilde{f}|) = I_{e_0}(\mathbf{x}; |\tilde{f}|) + \sum_{e \in F} I_e(\mathbf{x}; |\tilde{f}|),$$

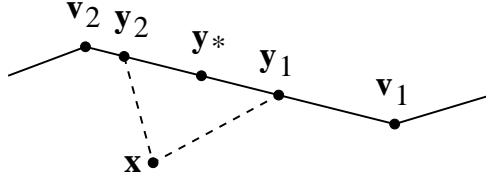


Figure 1: Interpolation at an edge point \mathbf{y}_* .

where

$$F = \{[\mathbf{v}_1, \mathbf{y}_1], [\mathbf{y}_2, \mathbf{v}_2]\} \cup (E \setminus [\mathbf{v}_1, \mathbf{v}_2]),$$

and it follows that $|g(\mathbf{x}) - f(\mathbf{y}_*)| \leq \gamma(\mathbf{x})/\phi(\mathbf{x})$, where

$$\gamma(\mathbf{x}) = \epsilon I_{e_0}(\mathbf{x}) + 2M \sum_{e \in F} I_e(\mathbf{x}),$$

and

$$M := \sup_{\mathbf{y} \in \partial\Omega} |f(\mathbf{y})|. \quad (5)$$

Similar to $\gamma(\mathbf{x})$, we can express $\phi(\mathbf{x})$ as

$$\phi(\mathbf{x}) = \tau_{e_0}(\mathbf{x}) I_{e_0}(\mathbf{x}) + \sum_{e \in F} \tau_e(\mathbf{x}) I_e(\mathbf{x}).$$

For \mathbf{x} close enough to \mathbf{y}_* , $\tau_{e_0}(\mathbf{x}) = 1$, and then

$$\frac{\gamma(\mathbf{x})}{\phi(\mathbf{x})} = \frac{\epsilon + 2M \sum_{e \in F} I_e(\mathbf{x})/I_{e_0}(\mathbf{x})}{1 + \sum_{e \in F} \tau_e(\mathbf{x}) I_e(\mathbf{x})/I_{e_0}(\mathbf{x})}.$$

As $\mathbf{x} \rightarrow \mathbf{y}_*$, $\alpha_{e_0}(\mathbf{x}) \rightarrow \pi$, and since $\mathbf{y}_* \notin e$ for all $e \in F$,

$$\alpha_e(\mathbf{x}) \rightarrow \alpha_e(\mathbf{y}_*) < \pi, \quad e \in F.$$

Therefore, by (3), as $\mathbf{x} \rightarrow \mathbf{y}_*$,

$$I_{e_0}(\mathbf{x}) \rightarrow \infty \quad \text{and} \quad I_e(\mathbf{x}) \rightarrow I_e(\mathbf{y}_*) \neq \infty, \quad e \in F.$$

Thus $\gamma(\mathbf{x})/\phi(\mathbf{x}) \rightarrow \epsilon$ as $\mathbf{x} \rightarrow \mathbf{y}_*$. Hence,

$$\limsup_{\mathbf{x} \rightarrow \mathbf{y}_*} |g(\mathbf{x}) - f(\mathbf{y}_*)| \leq \epsilon$$

for any $\epsilon > 0$ which shows that $|g(\mathbf{x}) - f(\mathbf{y}_*)| \rightarrow 0$ as $\mathbf{x} \rightarrow \mathbf{y}_*$. \square

4 Interpolation at a vertex

Theorem 2 For $\mathbf{v} \in V$, $g(\mathbf{x}) \rightarrow f(\mathbf{v})$ as $\mathbf{x} \rightarrow \mathbf{v}$ for $\mathbf{x} \in \Omega$.

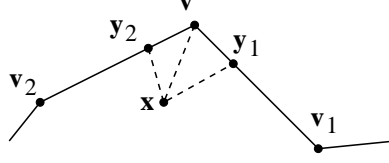


Figure 2: Interpolation at a convex vertex \mathbf{v} .

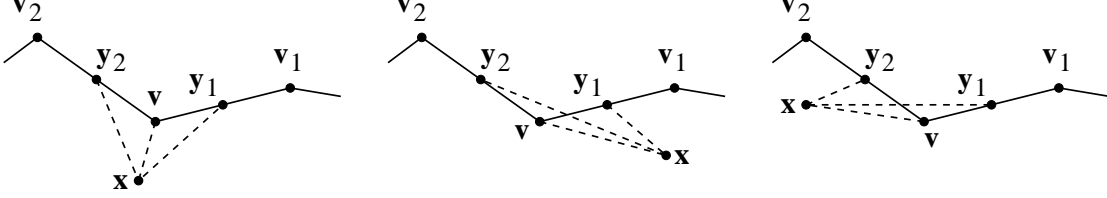


Figure 3: Interpolation at a concave vertex \mathbf{v} .

Proof. Similar to (4), from the form of (1),

$$|g(\mathbf{x}) - f(\mathbf{v})| \leq \sum_{e \in E} I_e(\mathbf{x}; |\tilde{f}|) / \phi(\mathbf{x}),$$

where $\tilde{f}(\mathbf{y}) := f(\mathbf{y}) - f(\mathbf{v})$.

Let \mathbf{v}_1 and \mathbf{v}_2 be the two neighbouring vertices of \mathbf{v} with $\mathbf{v}_1, \mathbf{v}, \mathbf{v}_2$ ordered anti-clockwise w.r.t. $\partial\Omega$ as in Figures 2 and 3. Let $\epsilon > 0$. By the continuity of f , there is some δ , where

$$0 < \delta < \min\{\|\mathbf{v}_1 - \mathbf{v}\|, \|\mathbf{v}_2 - \mathbf{v}\|\},$$

such that if \mathbf{y} is in $[\mathbf{v}_1, \mathbf{v}]$ or $[\mathbf{v}, \mathbf{v}_2]$ and $\|\mathbf{y} - \mathbf{v}\| \leq \delta$ then $|f(\mathbf{y}) - f(\mathbf{v})| < \epsilon$. Let $\mathbf{y}_j \in [\mathbf{v}, \mathbf{v}_j]$, $j = 1, 2$, be the point such that $\|\mathbf{y}_j - \mathbf{v}\| = \delta$, and define $e_1 = [\mathbf{y}_1, \mathbf{v}]$ and $e_2 = [\mathbf{v}, \mathbf{y}_2]$. Then,

$$\sum_{e \in E} I_e(\mathbf{x}; |\tilde{f}|) = I_{e_1}(\mathbf{x}; |\tilde{f}|) + I_{e_2}(\mathbf{x}; |\tilde{f}|) + \sum_{e \in F} I_e(\mathbf{x}; |\tilde{f}|),$$

where

$$F = \{[\mathbf{v}_1, \mathbf{y}_1], [\mathbf{y}_2, \mathbf{v}_2]\} \cup (E \setminus \{[\mathbf{v}_1, \mathbf{v}], [\mathbf{v}, \mathbf{v}_2]\}).$$

It follows that $|g(\mathbf{x}) - f(\mathbf{y}_*)| \leq \gamma(\mathbf{x}) / \phi(\mathbf{x})$, where

$$\gamma(\mathbf{x}) = \epsilon(I_{e_1}(\mathbf{x}) + I_{e_2}(\mathbf{x})) + 2M \sum_{e \in F} I_e(\mathbf{x}),$$

and M is as in (5). We can similarly express $\phi(\mathbf{x})$ as

$$\phi(\mathbf{x}) = \tau_{e_1}(\mathbf{x})I_{e_1}(\mathbf{x}) + \tau_{e_2}(\mathbf{x})I_{e_2}(\mathbf{x}) + \sum_{e \in F} \tau_e(\mathbf{x})I_e(\mathbf{x}).$$

Then using (3), and multiplying both $\gamma(\mathbf{x})$ and $\phi(\mathbf{x})$ by $\|\mathbf{v} - \mathbf{x}\|$, we have

$$\frac{\gamma(\mathbf{x})}{\phi(\mathbf{x})} = \frac{\epsilon(\tan(\alpha_{e_1}(\mathbf{x})/2) + \tan(\alpha_{e_2}(\mathbf{x})/2)) + A(\mathbf{x})}{\tau_{e_1}(\mathbf{x})\tan(\alpha_{e_1}(\mathbf{x})/2) + \tau_{e_2}(\mathbf{x})\tan(\alpha_{e_2}(\mathbf{x})/2) + B(\mathbf{x})},$$

where $A(\mathbf{x}), B(\mathbf{x}) \rightarrow 0$ as $\mathbf{x} \rightarrow \mathbf{v}$. Letting $\tau_j = \tau_{e_j}$ and $\alpha_j = \alpha_{e_j}$, $j = 1, 2$, and using the fact that $-\tan(\beta) = \tan(-\beta)$ for $\beta \in \mathbb{R}$, we can rewrite this as

$$\frac{\gamma(\mathbf{x})}{\phi(\mathbf{x})} = \frac{\epsilon(\tan(\alpha_1(\mathbf{x})/2) + \tan(\alpha_2(\mathbf{x})/2)) + A(\mathbf{x})}{\tan(\tau_1(\mathbf{x})\alpha_1(\mathbf{x})/2) + \tan(\tau_2(\mathbf{x})\alpha_2(\mathbf{x})/2) + B(\mathbf{x})}.$$

Next, using the identity

$$\tan(\beta_1) + \tan(\beta_2) = \frac{\sin(\beta_1 + \beta_2)}{\cos(\beta_1)\cos(\beta_2)},$$

and the fact that $\cos(-\beta) = \cos(\beta)$, it follows that

$$\frac{\gamma(\mathbf{x})}{\phi(\mathbf{x})} = \frac{\epsilon \sin((\alpha_1(\mathbf{x}) + \alpha_2(\mathbf{x}))/2) + \tilde{A}(\mathbf{x})}{\sin((\tau_1(\mathbf{x})\alpha_1(\mathbf{x}) + \tau_2(\mathbf{x})\alpha_2(\mathbf{x}))/2) + \tilde{B}(\mathbf{x})},$$

where

$$\begin{aligned}\tilde{A}(\mathbf{x}) &= \cos((\alpha_1(\mathbf{x})/2) \cos((\alpha_2(\mathbf{x})/2) A(\mathbf{x}), \\ \tilde{B}(\mathbf{x}) &= \cos((\alpha_1(\mathbf{x})/2) \cos((\alpha_2(\mathbf{x})/2) B(\mathbf{x}),\end{aligned}$$

and so also $\tilde{A}(\mathbf{x}), \tilde{B}(\mathbf{x}) \rightarrow 0$ as $\mathbf{x} \rightarrow \mathbf{v}$.

Finally, we consider the two cases (i) \mathbf{v} is a convex vertex and (ii) \mathbf{v} is a concave vertex. In case (i), referring to Figure 2 we see that for \mathbf{x} close enough to \mathbf{v} , $\tau_1(\mathbf{x}) = \tau_2(\mathbf{x}) = 1$ and so

$$\lim_{\mathbf{x} \rightarrow \mathbf{v}} \frac{\gamma(\mathbf{x})}{\phi(\mathbf{x})} = \epsilon. \quad (6)$$

In case (ii), the values of $\tau_1(\mathbf{x})$ and $\tau_2(\mathbf{x})$ depend on the location of \mathbf{x} , even when \mathbf{x} is close to \mathbf{v} . However, for any \mathbf{x} that is close enough to \mathbf{v} , we have the identity (observed in [6])

$$\tau_1(\mathbf{x})\alpha_1(\mathbf{x}) + \tau_2(\mathbf{x})\alpha_2(\mathbf{x}) = \alpha_{[y_1, y_2]}(\mathbf{x}).$$

This can be verified in the three cases illustrated in Figure 3. In the three configurations, from left to right, we have, respectively,

$$\alpha_{[y_1, y_2]}(\mathbf{x}) = \begin{cases} \alpha_1(\mathbf{x}) + \alpha_2(\mathbf{x}), \\ \alpha_1(\mathbf{x}) - \alpha_2(\mathbf{x}), \\ -\alpha_1(\mathbf{x}) + \alpha_2(\mathbf{x}). \end{cases}$$

Thus,

$$\lim_{\mathbf{x} \rightarrow \mathbf{v}} (\tau_1(\mathbf{x})\alpha_1(\mathbf{x}) + \tau_2(\mathbf{x})\alpha_2(\mathbf{x})) = \alpha_{[y_1, y_2]}(\mathbf{v}) = \alpha_{[v_1, v_2]}(\mathbf{v}) \in (0, \pi).$$

Since $\sin((\alpha_1(\mathbf{x}) + \alpha_2(\mathbf{x}))/2) \leq 1$, it follows that in case (ii),

$$\limsup_{\mathbf{x} \rightarrow \mathbf{v}} \frac{\gamma(\mathbf{x})}{\phi(\mathbf{x})} \leq \frac{\epsilon}{\sin(\alpha_{[v_1, v_2]}(\mathbf{v})/2)}. \quad (7)$$

From (6) and (7) we deduce that for any type of vertex \mathbf{v} , $|g(\mathbf{x}) - f(\mathbf{v})| \rightarrow 0$ as $\mathbf{x} \rightarrow \mathbf{v}$. \square

5 Numerical examples

In this section we present two examples of transfinite mean value interpolants of different functions $f(x, y)$ over a polygonal-shaped domain in order to confirm the theoretical interpolation property proven in Sections 3 and 4. For the implementation we have evaluated the mean value interpolant $g(x, y)$ using the boundary integral formula of [1]. This is more efficient than applying the definition, equation (1), which would require computing intersection points.

The first function we consider is

$$f(x, y) = x^2 - y^2$$

defined on the non-convex polygon in Figure 4a. Figures 4a and 4b illustrate the exact surface and Figures 4c and 4d the corresponding interpolant $g(x, y)$. Figure 4e shows the absolute error $|f(x, y) - g(x, y)|$. The darker the colour the smaller the error and, as expected, the error vanishes as we get close to the boundary.

For our second example we chose the function

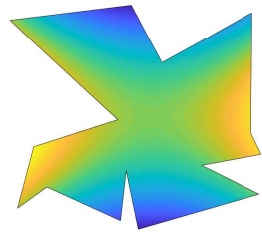
$$f(x, y) = \frac{1}{9}[\tanh(9x - 9y) + 1].$$

Figures 5a and 5b and Figures 5c and 5d show the exact surface and the interpolant, respectively, while Figure 5e shows the absolute error.

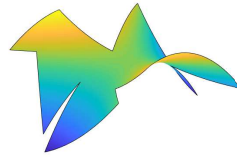
Acknowledgement. This project has received funding from the European Union’s Horizon 2020 research and innovation programme under the Marie Skłodowska-Curie grant agreement No 675789.

References

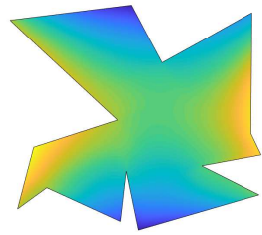
- [1] C. Dyken and M. S. Floater, *Transfinite mean value interpolation*, *Comput. Aided Geom. Design* **26** (2009), 117–134.
- [2] M. S. Floater, *Mean value coordinates*, *Comput. Aided Geom. Design* **20** (2003), 19–27.
- [3] ———, *Generalized barycentric coordinates and applications*, *Acta Numerica* **24** (2015), 161–214.
- [4] M. S. Floater, K. Hormann, and G. Kós, *A general construction of barycentric coordinates over convex polygons*, *Adv. Comput. Math.* **24** (2006), 311–331.
- [5] M. S. Floater, G. Kos, and M. Reimers, *Mean value coordinates in 3D*, *Comput. Aided Geom. Design* **22** (2005), 623–631.
- [6] K. Hormann and M. S. Floater, *Mean value coordinates for arbitrary planar polygons*, *ACM Trans. on Graph.* **25** (2006), 1424–1441.
- [7] T. Ju, S. Schaefer, and J. Warren, *Mean value coordinates for closed triangular meshes*, *ACM Trans. on Graph.* **24** (2005), 561–566.



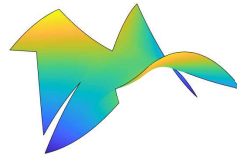
(a)



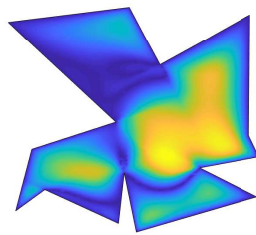
(b)



(c)

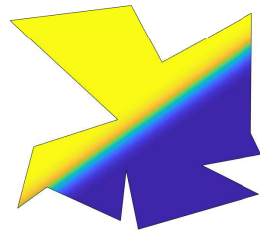


(d)

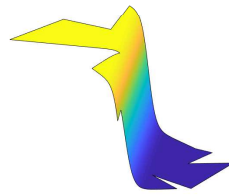


(e)

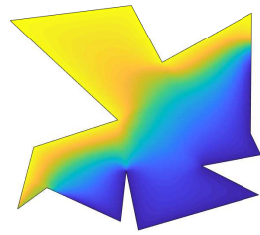
Figure 4



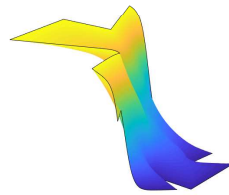
(a)



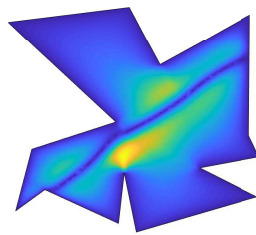
(b)



(c)



(d)



(e)

Figure 5

